Proceedings of ASME Turbo Expo 2011
GT2011
June 6-10, 2011, Vancouver, British Columbia, Canada

GT2011-45965

Dynamic Characteristics of Dry Friction Damping at Bladed Disk Joints: Experiments

Hong Jie, Chen Lulu, Ma Yanhong, Zhang Dayi
School of Jet Propulsion, Beihang University

Mail Address: 405 Group, Beihang University, Beijing 100191 PR. China
Tel: +86-10-82339012; E-mail Address: hongjie@buaa.edu.cn

ABSTRACT
An experimental system was designed to measure dynamic responses of non-rotating blade, in which the similar stress and strain fields can be recreated similar to a blade which is fixed to its disk by means of dovetail. During the experiments, the beam was subject to different tensile loads and excitation forces. The dynamic response was measured while the beam was vibrating as various modes. The effects of tensile load, excitation load and contact condition at bladed disk joints on the resonance frequency and resonance response level were analyzed from the test results. These results could be used to explain the measured dynamical response in view of the behavior at the interface.

1 INTRODUCTION
Blade is a critical aero-engine component. Many serious flight accidents are caused by the failure of blade. High-cycle fatigue failure is the main mode which is caused by forced vibration. Due to the high mode density of natural frequencies of realistic bladed disks and a broad spectrum of aerodynamic excitation forces, complete prevention of the occurrence of resonance regimes is not feasible. So it is a problem of major practical importance to develop methods in order to provide accurate, fast and robust predictive tools for the analysis of forced vibration response levels of bladed disks under operating conditions.
Accuracy of prediction of forced response levels is dependent on the accurate dynamic model of bladed disk components. Damping and stiffness of the bladed disk joints are among the uncertainties of such models. Two of the most commonly used blade-disk attachment geometries are the dovetail and the fir-tree types. The blade is subject to the centrifugal load and thermal load under operating conditions. These loads are supported by the large contact areas between blade and disk. Usually such contact areas are considered ideal constraints which prevent any relative motion. In the case of blade vibration, the joint supports cyclic loads superimposed on the centrifugal load. The actual distribution of contact pressure and tangential stresses due to the vibrations may generate some sliding limited to part of the contact: microslip. Microslip reduces the actual stiffness of the joints, affecting the resonance frequencies of the system. Demands to increase the accuracy of predictive analysis methods require development of advanced model including the interaction at joints of blade-disk, especially at low rotational speeds and high excitation levels. Additionally microslip can generate friction damping and affect the resonance response level. The general rule is to include in the dynamic model of the blade a viscous damping ratio which accounts for the material damping, viscous damping and the hysteretic damping at the blade-disk joint. Such damping is usually considered constant for different engine rotational speeds and also constant for the whole life of the engine. Additionally, the value of the damping ratio is sometimes based on tradition or routine since no verified models are yet able to predict the damping in real engine conditions and no experimental data are available. But the friction damping is different under different rotational speeds and excitation levels in real engine. The main factors of friction damping include: static loads, amplitude of the dynamic forces, material properties, contact history and so on. The contact interaction forces have a strongly nonlinear character due to: slip-stick transitions, variation of contact area during each cycle of vibration, and others. Because of the uncertain characteristic, such as the strong nonlinearity, various contact condition and the wear, the problem of developing methods in order to obtain accurate models for the analysis of forced vibration

response levels of bladed disks is a difficult problem for the designers.

The researchers have conducted a large number of theoretical researches. Several kinds of friction contact models, including one-dimensional, two-dimensional and three-dimensional[1,2,3], are put forward to investigate the contact kinematics at the interfaces, series and parallel models[4] are conducted to describe the contact condition, and the methods to predict the nonlinear response level of frictionally constrained blade systems are advanced[5,6,7]. But many assumptions are applied because of the serious nonlinearity of contact problems. Besides many key parameters are varying with time during vibratory courses, such as contact stiffness, friction coefficient and etc. Thus it is necessary to do some experimental study. The model and analytic method will be improved based on test results and test data.

Therefore, the researchers have conducted a large number of experimental researches. An experimental instruments was designed to measure the contact stiffness and friction coefficient by Schwingshackl[8]. The relationship between the damping capacity of paired shrouded blade and the shroud contact conditions were investigated by Matveev[9]. The result was obtained which reflect regularities in the variation of blade vibration decrement in relation to the amplitude of dynamic bending stress. Pfeiffer and Hajek[10] also did some experimental research on the underplatform damper with various geometries showing curved or flat surfaces. Shangguan Bo and Marco Allara had do some experimental research on the friction damping at bladed disk joints, respectively [11,12]. The dynamic responses of a group of simulation blades with different dovetail attachment angles were measured in consideration of variable simulation centrifugal force by Shangguan Bo. The dynamic responses of plane blades for different vibration mode were measured when the centrifugal force and excitation level are variable by Marco Allara. But the effect on contact conditions, which is important to evaluate friction damping were not considered in their researches. A rotating bladed disk was tested in a vacuum chamber by D. Charleux and C. Gibert[13]. Nonlinear behavior observed experimentally at resonances was well reproduced and an acceptable correlation was found with experimental resonant frequencies, amplitudes, and amount of damping throughout the spinning speed and excitation level range.

An experimental system was designed to measure dynamic responses of non-rotating blade, in which the similar stress and strain fields can be recreated similar to a blade which is fixed to its disk by means of dovetail. During the experiments, the specimens were subject to different tensile load and excitation force. The dynamic responses were measured while the specimens were vibrating as various modes. The effects of tensile loads, excitation loads and contact condition at bladed disk joints on the resonance frequency and resonance response level were analyzed from the test results. These results could be used to explain the measured dynamical response in view of the behavior at the interface.

2 EXPERIMENTAL SYSTEM

An experimental system was designed to measure dynamic responses of non-rotating blade, in which the similar stress and strain fields can be recreated similar to a blade which is fixed to its disk by means of dovetail. Its configuration is shown in Fig.1. It includes three parts: tensile loading rig, specimens, excitation and measurement system.

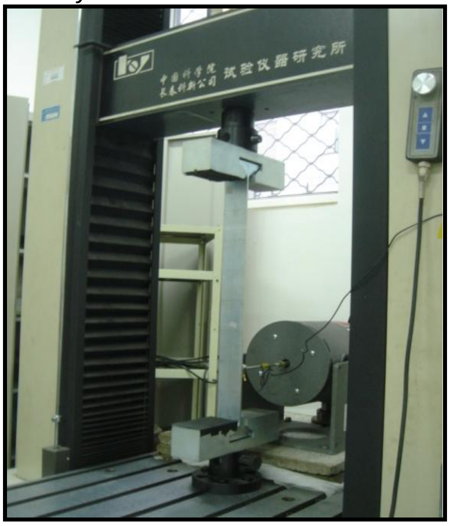

Fig.1 Experimental system

2.1 Tensile loading rig

WDW3100 electronic testing machine was used to provide the necessary tensile load as shown in Fig.2. It consisted of moving crossbar, test bench and external frame. The joint components were designed to fix two mortises on the moving crossbar and test bench. The force sensor was fixed on the moving crossbar to obtain the value of tensile force. The measuring range of force sensor is 120N~30kN, and the precision of prescribed load is 0.5%.

2.2 Specimens

One beam was designed during study as shown in Fig.1. The material of beam was stainless steel; its frame size was 450mm×50mm×3mm. The friction coefficient is assumed as 0.3. The size of the total contact area between the dovetail and the groove is 8000mm^2 and the dovetail angle is 45°. The section of beam was designed to be flat because the plane blade was easy to machine and the characteristics of forced responses were easy to master. In order to focus on the behavior of the joints, both ends of the beam were machined in the shape of a dovetail blade root[11]. This geometry was selected to avoid the introduction of any other source of damping. This assembly was close to those of a real blade. The beam was machined out of hardened steel in order to supply enough stiffness and hardness.

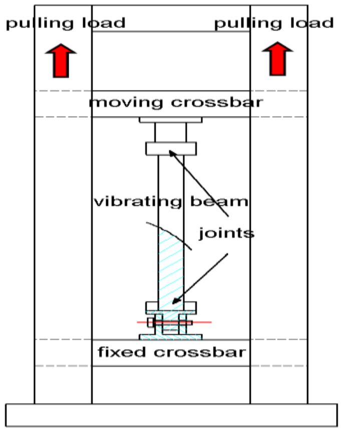

Fig.2 Tensile load rig

The excitation mortise is shown in Fig.3. During the operation, real blade is subject to the centrifugal load and thermal load. These loads are supported by the large contact areas between blade and disk. On a real bladed disk, the circumferential components of the static contact forces that one blade root exerts upon the disk are in equilibrium with those of the adjacent blades. In the experiment, only one specimen is present, so the circumferential components may bend the slot sides opening the slot and changing the contact geometry. To reduce this effect, the sides of the slot in the experiment were extended and thicken.

Fig.3 Experimental mortise

2.3 Excitation and measurement system

The excitation and measurement systems are shown in Fig.4. The sine signal emitted from the signal generator is magnified through the power amplifier, and the shaker is driven by the amplified signal, then the shaker excites the beam through push rod. The force sensor is fixed on the push rod to obtain the value of the excitation force. The intensities of signal generator and power amplifier can be adjusted by manual operation before testing so that an appropriate value of the excitation force is chosen, and during testing the excitation force can be regarded as invariable.

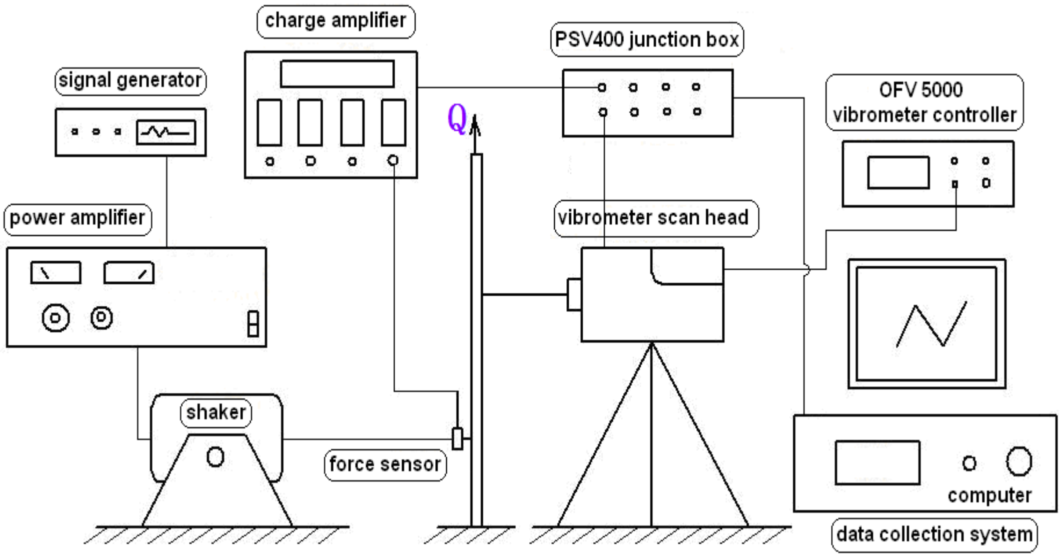

Fig.4 Excitation and measurement system

Non-contact scanning vibrometer is used to measure the vibration velocity and dynamics characteristics of the beam. The distributions of pickup points and excited point are shown in Fig.5. The signals gained from force sensor and laser sensor are transferred into voltage through the junction box, then the signals are collected by the data collection system. In order to obtain the effects of tensile load and excitation load on the resonance frequency and damping obviously, the responses of beam vibrating as the first three modes are studied.

2.4 Experimental errors analysis

The experimental errors rooted in the reasons were as follows:

Firstly, the errors of additional damping were caused by the contact between component joints. So contact joints between the two mortises and tensile loading rig were designed to be interference fit in order to reduce the additional damping.

Secondly, the errors of readings and measurement system caused stochastic errors, i.e., there would be errors unavoidably during adjusting excitation force and reading result. So experiment was handled repetitiously in order to reduce these errors.

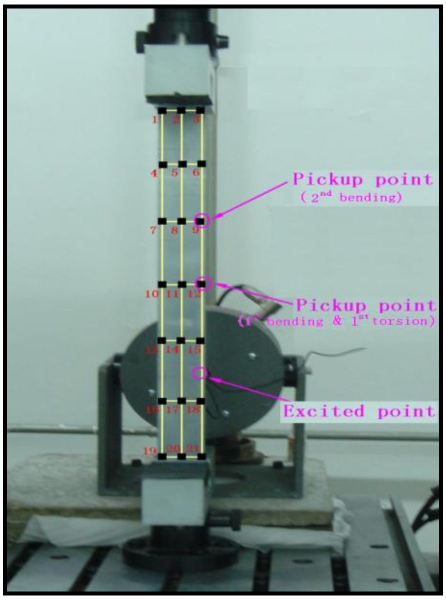

Fig. 5 Excited and pickup points

3 EXPERIMENTAL CONTENTS AND PROCESSES

3.1 Experimental contents

The experimental contents were as follows:

1) The amplitude-frequency responses were obtained while the excitation level was different. The effects of the amplitude of excitation force on resonance frequency, damping ratio and contact conditions (which are presented with the numerical model and experimental data) were analyzed.

2) The amplitude-frequency responses were obtained while the value of tensile load was different. The effects of the amplitude of tensile load on resonance frequency, damping ratio and contact conditions were analyzed.

3) All these were measured while the beam was vibrating as 1^{st} bending mode, 2^{nd} bending mode and 1^{st} torsion mode. Thus the effect of the resonance mode is also analyzed.

3.2 Experimental processes

The experimental processes were as follows:

1）Fixing the plane blade. Firstly, two clamps were fixed on the moving crossbar and test bench, respectively. The mortises were fixed on the clamps through pins. Secondly, the height of the moving crossbar was adjusted to cooperate with the length of the beam. The beam was fixed on the test rig after adjusting. Then the height of the moving crossbar was fine-tuned to make the beam stationary.

2）Forcing tensile load. The value of tensile load was obtained by the force sensor which was fixed on the moving crossbar.

3）Measuring response level. The amplitude-frequency responses at 21 points of the beam were measured while the exciting frequency was increasing. During the test, the excitation level could be regarded as invariable. The response was measured after the signal appeared to be stability at each frequency.

The amplitude-frequency response under certain tensile load and excitation load was obtained through the experimental processes above. The amplitude-frequency response under altering loads above could be acquired by repeating some of the process.

4 DATA PROCESSING

During the data processing, ANSYS is used to obtain the distribution of contact conditions. The version number of the FE code is 11.0.

Firstly, the finite element model was established which is shown in Fig.6. Element 45 is used in the FE model which contains 10989 DOFs and 8490 elements in the calculation. The contact areas of upper dovetail were defined to be interface A and interface B, respectively. Point C was defined as a monitoring point which is on the interface A.

Secondly, the initial contact conditions were obtained by static analysis. During the static calculation, the lower dovetail was defined to be stationary, and the upper dovetail was defined to be subject the tensile load. The interfaces between the tongues and grooves were defined to be contact pairs. The contact algorithm is Augmented Lagrange method. These boundary conditions are as shown in Fig.7.

Thirdly, the transient analysis was conducted. The boundary conditions were changed in transient analysis in order to improve the convergence. And the static results were used as pre-stress during transient analysis. 21 points on the beam were applied the test results. These boundary conditions are as shown in Fig. 8. The time steps and cycles were defined according to the tested resonance frequency.

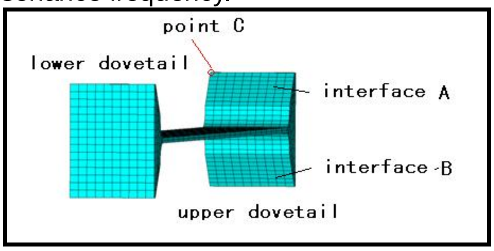

Fig.6 Finite element model

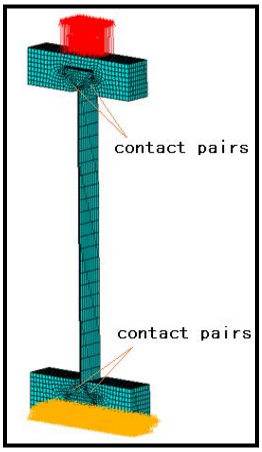

Fig. 7 Static model

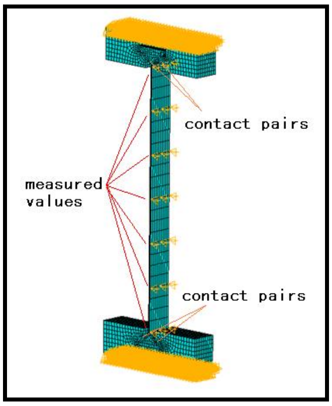

Fig.8 Transient model

5 RESULTS

The experimental curves are indicated as follows partially, thus the effects of the interaction at bladed disk joints on the resonance frequency and response level are gained from studying the experimental curves. The velocity can be obtained directly by means of laser vibrometer. The response with displacement unit needs to be calculated through the post-processing. And both the response with velocity unit and the one with displacement unit have similar characteristics.

5.1 Effect of Excitation Level on Resonance Frequencies

The effects of excitation level on dynamic characteristics are analyzed from test results. In order to clearly demonstrate the nonlinear dependency of this amplitude to excitation levels, it is normalized by dividing by Kf. Position of the excitation loads over the blade in all cases was the same, and these loads are multiplied by a factor Kf with values from 0.7% to 20%. The amplitude-frequency curve and resonance frequency varying with excitation level are plotted in Fig. 9 while the value of tensile load is 1000N and the beam is vibrating as 1st bending mode. Finite Element Method is used to calculate the modal frequencies as a function of the tensile load. The analytic results are also compared in Fig.9.

From Fig.9a, one can see that the response level increases with the increase of the excitation level and the resonance frequencies are different for these cases. The resonance frequency was obtained according to the measured Amplitude-Frequency curve. The effect of the excitation level on the resonance frequency is demonstrated in Fig. 9b. When the level of relative displacement is too small to cause slip at the interfaces or variation of the contact conditions, the resonance frequency is very close to resonance frequency of the linear system with the ideal constraint. But with the increase of the relative displacement, the resonance frequency decreases. There is more than 13% shift between these cases when the excitation level changes. The resonance frequency cannot be considered constant.

It is properly due to that when the excitation level is small the contact condition is mainly stick and the tested results are close to the numerical results for this case. With the increase of the excitation level, the relative displacement increases and it causes part of contact area begin to slip which was going to be studied by means of the numerical model based on the test data. The contact stiffness decreases with the occurrence of slipping.

The effect of vibrating mode is demonstrated in Fig. 10 for a frequency range including 2nd bending mode, and in Fig. 11 for a frequency range including 1st torsion mode. Position of the excitation loads in all cases was the same. One can see that, the resonance frequency is unchanged for torsion mode, and that is different from bending mode.

This is because the component of relative displacement in the tangential direction is much larger than the one in the vertical direction when the beam is vibrating as bending mode. The components in the tangential and vertical direction affect the condition of slip-stick transition at the interfaces, and the contact conditions affect the contact stiffness and damping.

5.2 Effect of Tensile Force on Resonance Frequency

The effect of the level of the tensile force on resonance frequency is demonstrated in Fig. 12 when the excitation level is the maximum value corresponding to 1st bending mode, 2nd bending mode and 1st torsion mode.

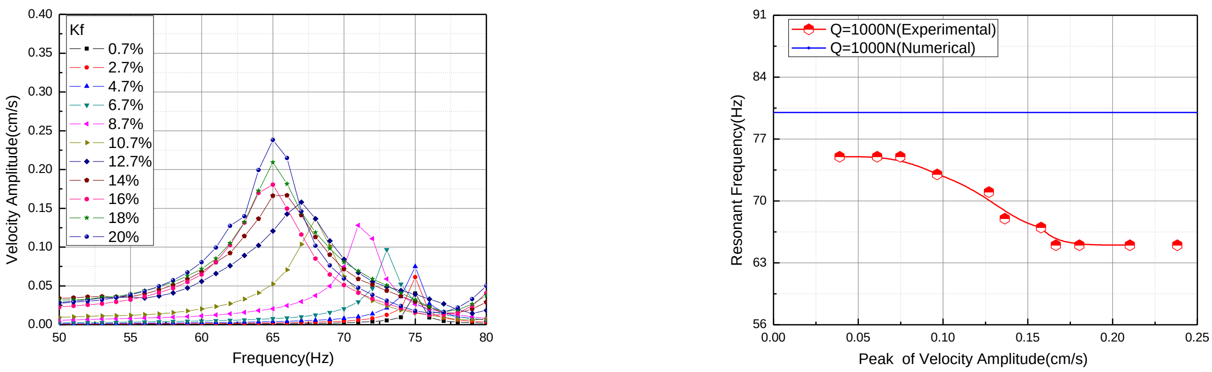

(a) Amplitude-frequency curve

(b) Resonance frequency varies as a function of response amplitude

Fig.9 1st bending mode

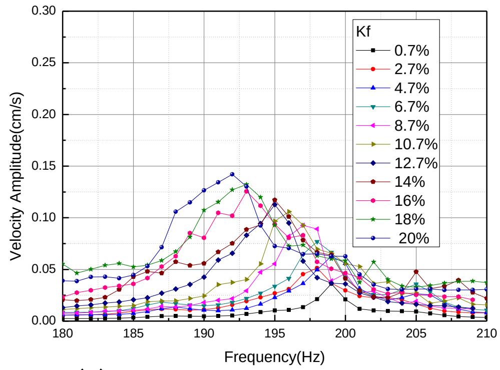

(a) Amplitude-frequency curve

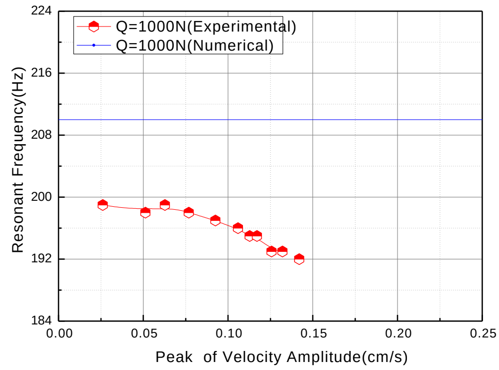

(b) Resonance frequency varies as a function of response amplitude

Fig.10 2nd bending mode

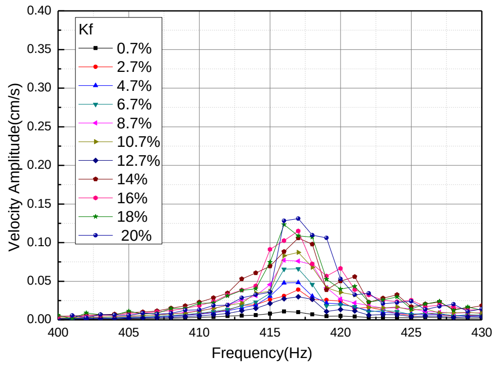

(a) Amplitude-frequency curve

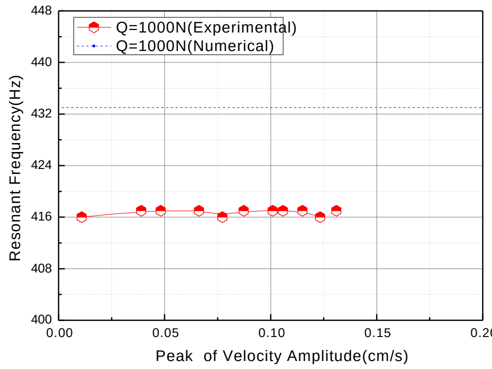

(b) Resonance frequency varies as a function of response amplitude

Fig.11 1st torsion mode

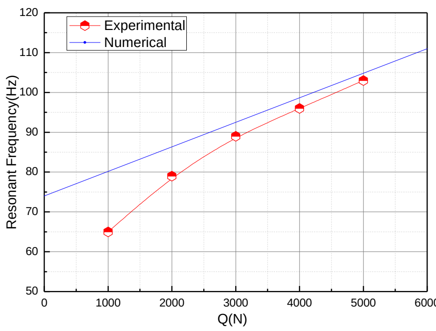

(a) 1st bending mode

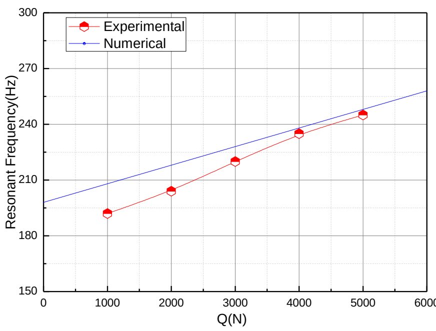

(b) 2nd bending mode

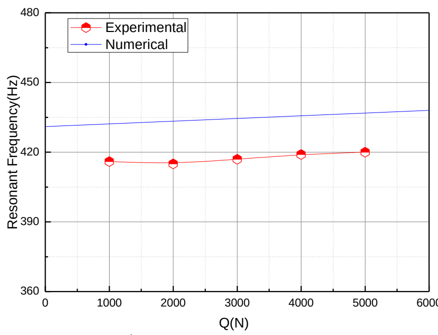

(c) 1st torsion mode

Fig.12 Resonance frequency varies as a function of tensile load

One can see that the resonance frequencies get close to the numerical result with the increase of tensile load for 1st bending mode and 2nd bending mode, but not for 1st torsion mode. This results from the fact that the amplitude and distribution of the relative displacement at the interface are among the factors influencing the transition condition of contact conditions. The slipping part of contact area decreases with decreasing the amplitude of vibrating displacement which is dependent on resonance frequency and vibration energy. Additional, the blade vibration for torsion mode mainly induce the relative motion in the vertical direction of blade-disk joints. The sliding which is mainly generated by the tangential vibrations rarely occurs.

5.3 Effect of Excitation Level on Damping

The effect of the excitation level on damping is demonstrated in Fig. 13 when the tensile load is different. The damping ratio is obtained by half-power method.

It can be seen from the figure:

1) When the tensile load is small, the damping ratio corresponding to bending mode firstly increases and then decreases with the increase of the vibration amplitude, and the maximum value is 0.04. When the tensile load is larger, the damping ratio also increases with the increase of the vibration amplitude, but the rate of increase is significantly reduced.

2) Compared with the bending modes, the damping ratio corresponding to torsional mode doesn't change.

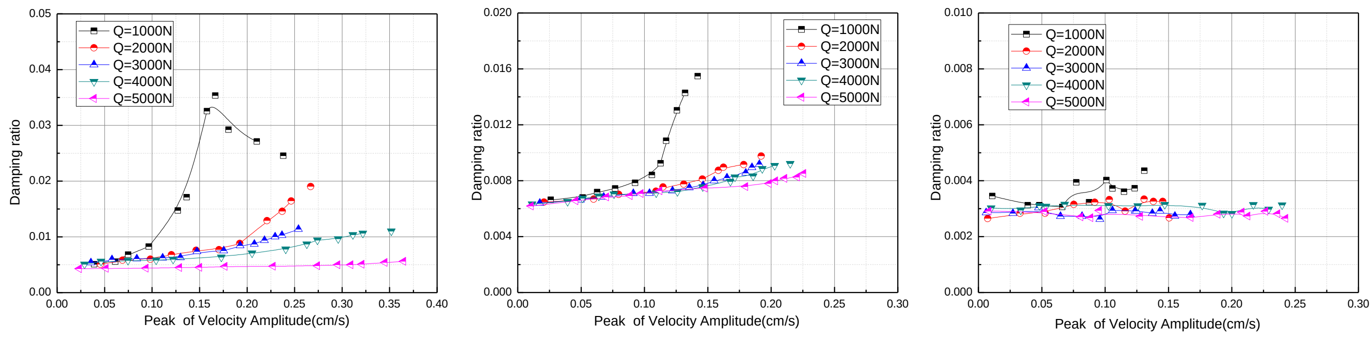

(a) 1st bending mode (b) 2nd bending mode (c) 1st torsion mode

Fig.13 Damping ratio varies as a function of response amplitude

5.4 Effect of Excitation Level on Contact Conditions

Contact conditions and parameters at the interface affect directly dry friction damping. But they often cannot be measured directly. In order to study the effects of relevant parameters on contact conditions, finite element method was used to obtain the distribution of contact conditions according to response level which was measured by Laser vibrometer.

The distribution of vibrating displacement for three different excitation levels at the measured resonance frequency was shown in Fig.14. From the figure, one can see that these vibrating modes are alike and the response level increases with the increase of excitation level. The contact conditions at interface A for three different excitation levels are shown in Fig.15. The symbol "T" was the period of the response. Three possible contact conditions are indicated by different colors: (i) a case with separation is colored blue, (ii) a case with stick is colored red, and (iii) a case with slip is colored orange. From this figure, one can see that the contact condition at interface A varies with time. The contact conditions are different when the relative displacements are different. For a case of 0.7% excitation level, majority of contact area is sticking or separating at the resonance frequency. The increase of excitation level increases the size of contact area where the slip-stick transition occurs. Based on the results of damping ratio, one can see that the friction damping also increases with the increase of excitation level. According to the damping ratio in Fig.13, one can see that the damping ratio increased with the increase of the region of stick-slip transition but not increased with the increase of the slip region. The contact pressure σ_n and friction stress σ_t of point C which has been indicated in Fig.15 are shown in Fig.16 and Fig.17. One can see that the stress varies periodically with the time. In Fig 17, the doted curve is represented the friction stress. Two other curves is represented the critical friction stress. The symbol ‘μ ’ was represented the friction coefficient. From Fig 17, one can see that three contact conditions occurred during a period, they were open corresponding to the friction stress equaled to zero, slip corresponding to the friction stress equaled to the critical friction stress and stick.

5.5 Effect of Vibration Mode on Contact Conditions

It is shown that the distribution of vibrating displacement for three different vibration mode in Fig.18. One can see that the vibration modes are respectively 1st bending mode, 2nd bending mode and 1st torsion mode. The contact conditions for different vibration mode are shown in Fig.19. One can see that the distributions of contact condition are very similar when the vibration mode is bending mode, and are very different from the one for torsion mode. This is really due to the amplitude and distribution of relative displacement which are decided by vibration mode.

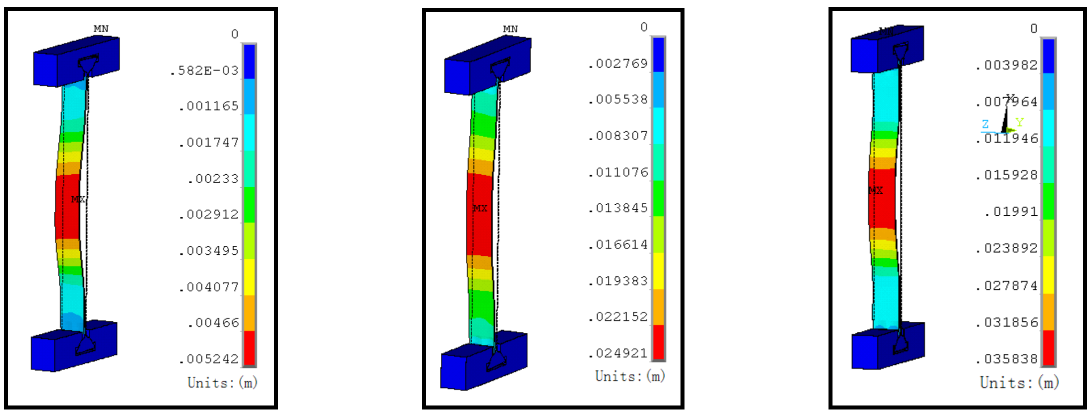

(a) Kf=0. 7% (b) Kf=14% (c) Kf=20%

Fig.14 Response levels while excitation level is different. (Q=1000N)

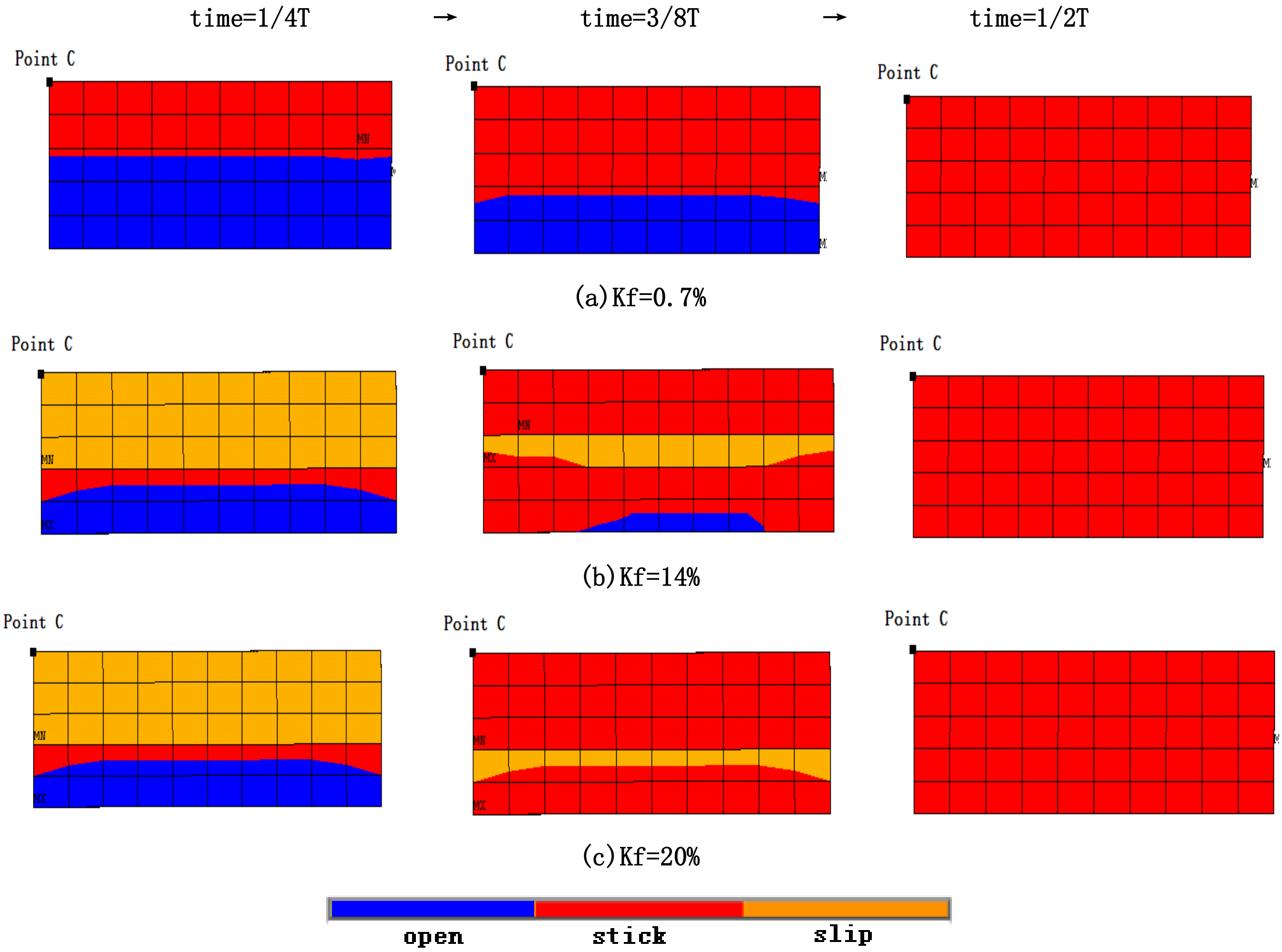

Fig. 15 Contact conditions while excitation level is different (Q=1000N)

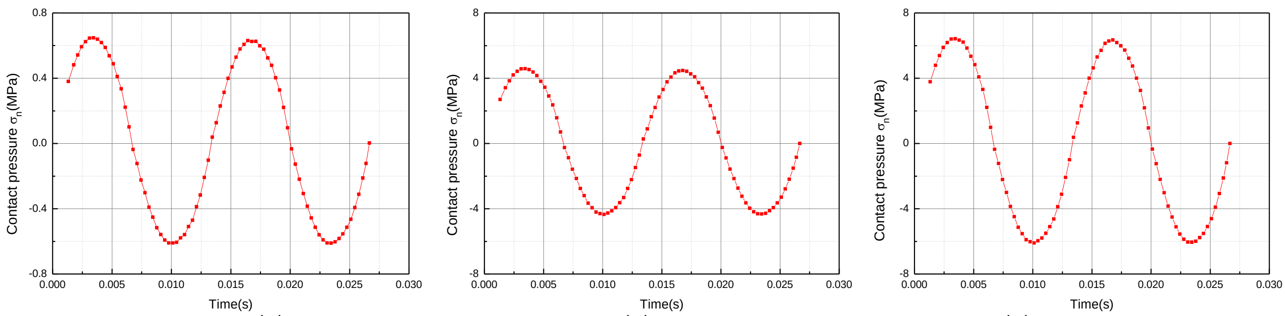

(a) Kf=0.7% (b) Kf=14% (c) Kf=20%

Fig.16 Contact pressure at point C while excitation level is different. (Q=1000N)

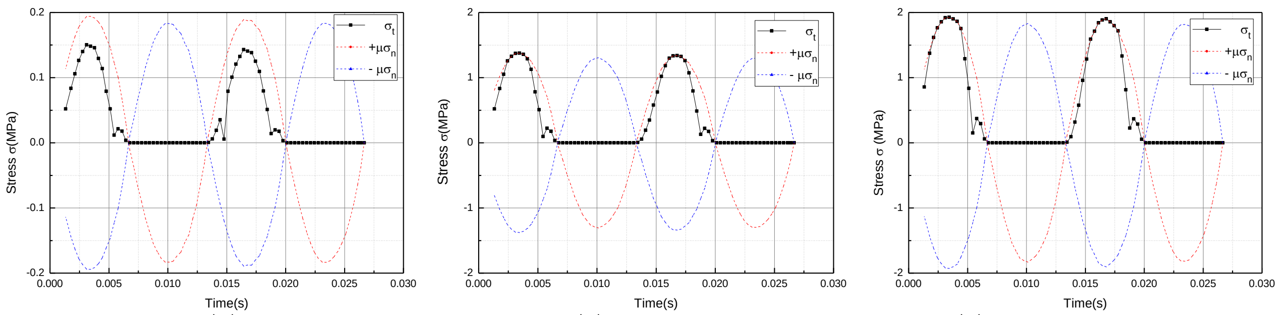

(a) Kf=0.7% (b) Kf=14% (c) Kf=20%

Fig.17 Friction stress at point C while excitation level is different. (Q=1000N)

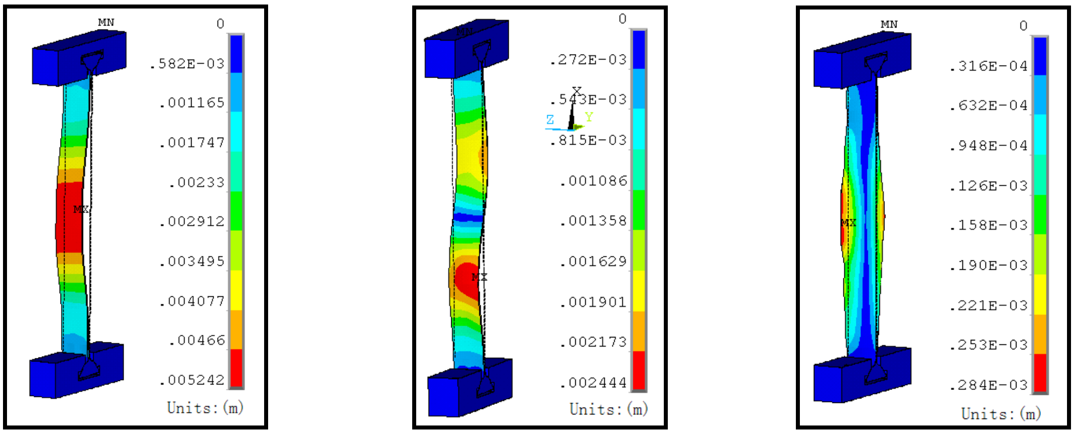

(a) 1st bending mode (b) 2nd bending mode (c) 1st torsion mode

Fig. 18 Response levels while vibrating mode is different. (Q=1000N, Kf=0.7%)

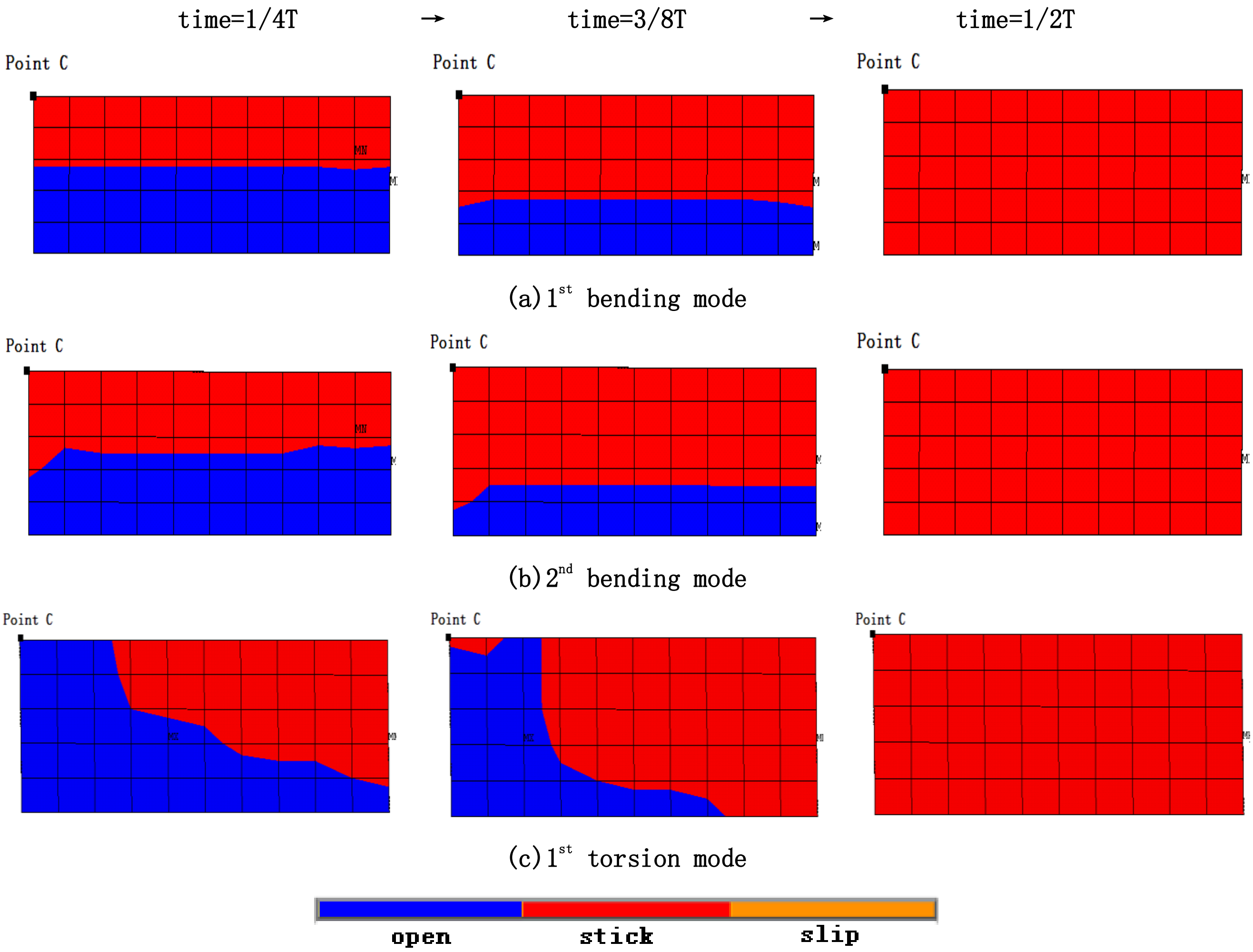

Fig. 19 Contact conditions while vibrating mode is different. (Q=1000N, Kf=0.7%)

6 CONCLUSIONS

An experiment method is developed to simulate the vibration of a gas turbine blade attached to the disk by means of dovetail. Amplitude-frequency and damping ratio are obtained for different tensile load, excitation level and various vibrating mode. Contact conditions are studied by means of the numerical model based on the test data. The following statements can be inferred from the experimental results:

Firstly, when the level of relative displacements is too small to cause slip at the interfaces or variation of the contact conditions, the resonance frequency is very close to the one of the linear system with the ideal constraint. But with the increase of the relative displacement, the resonance frequency varies. There is more than 13% shift between these cases when the excitation level is different. The resonance frequency

cannot be considered constant, especially for the bending mode.
Secondly, when the tensile load is smaller or the vibration amplitude is larger, the contact condition at blade root affects the damping of the system. The damping is not only from the structure itself, and the friction damping at the interfaces cannot be ignored. The damping for bending mode has more obvious changes than torsion mode.
Finally, when the system is vibrating, the contact pressure varies periodically. The tensile load, excitation level and vibrating mode affect the amplitude a components of relative displacement in the tangential and vertical direction, and it affect the distribution of contact conditions which affect the contact stiffness and friction damping.

NOMENCLATURE

Kf Excitation Factor
Q Tensile Loads
T Vibration Cycles
σ_n Contact Pressure
σ_t Friction Stress
μ Friction Coefficient

REFRENCES

[1]Cameron T. M., Griffin J. H., Kielb R. E., An Integrated Approach for Friction Damper Design[J]. Journal of Vibration, Acoustics, Stress, and Reliability in Design, 1990, Vol.112: 175-182

[2]Sanliturk, Ewins, Modeling Two-Dimensional Friction Contact and Its Application Using Harmonic Balance Method[J]. J. Sound and Vibration, 1996，Vol.193(2): 511-523

[3]Yang B. D., Menq C. H., Characterization of 3D Contact Kinematics and Prediction of Resonance Response of Structure Having 3D Friction Constraint[J]. Journal of Sound and Vibration, 1998, Vol.217(5): 909-925

[4]Iwan W. D., On a Class of Models for the Yielding Behavior of Continuous and Composite Systems[J]. ASME Journal of Applied Mechanics, 1967, Vol.89: 612-617

[5]Dowell E. H. and Schwartz H. B., Forced Response of a Cantilever Beam With a Dry Friction Damper Attached Part II: Experiment[J]. Journal of Sound and Vibration, 1983, Vol.91(2): 269-291

[6]Earles S. W. and Williams E. J., A Linearized Analysis of Frictionally Damped Systems[J]. Journal of Sound and Vibration, 1972, Vol. 24 (4): 445-458

[7]]Meng C. H., Griffin J. H., Bielak J., The Forced Response of Shrouded Fan Stages[J]. ASME Journal of Vibration, Acoustics, Stress, and Reliability in Design, 1986, Vol.108: 50-55

[8]C. W. Schwingshackl, E. P. Petrov, Validation of Test Rig Measurements and Prediction Tools For Friction Interface Modeling[A]. Proceeding of ASME Turbo Expo 2010 Power for Land, Sea, and Air[C], June 14-18, 2010, Glasgow, UK, GT2010-23274

[9]V. V. Matveev, I. G. Tokar, S. S. Gorodetskii, A. B. Roitman, Damping Capacity of Paired Shrouded Turbine Blades in Relation to Shroud Contact Conditions, 1978

[10]Pfeiffer F., Hajek M., Stick-Slip Motion of Turbine Blade Dampers[G]. Philosophical Transactions of the Royal Society of London, Series A, 1992, Vol.338(1651): 503-517

[11]Marco Allara, Sergio Filippi and Muzio M. Gola, An experimental Method for the Measurement of Blade-Root Damping, Proceeding of ASME Turbo Expo 2006 Power for Land, Sea, and Air[C]. GT2006-90774.

[12]Shangguan Bo, Xu Zili, Liu Yalin and Xu An, Experimental Investigation on Damping Characteristics of Blade with Loosely Assembled Dovetail Attachment, Proceeding of ASME Turbo Expo 2010 Power for Land, Sea, and Air[C], GT2010-22386.

[13] D. Charleux, C. Gibert, F. Thouverez and J. Dupeux，Numerical and Experimental Study of Friction Damping in Blade Attachments of Rotating Bladed Disks，International Journal of Rotating Machinery，2006，Vol: 1–13

